

A case of iniencephaly in a 36 week-old human female fetus

Ernest F. Talarico, Jr.,¹ and Theodore M. Hiemstra²

¹Anatomy & Cell Biology, Indiana University School of Medicine-Northwest, Gary, Indiana, USA

²Department of Biological Sciences, Purdue University Calumet, Hammond, Indiana, USA

SUMMARY

The purpose of this investigation was to characterize iniencephaly, a neural tube defect (NTD), in a 36-38 week-old human female fetus. Iniencephaly is a fatal, anatomic anomaly that lacks a direct etiology. However, multiple factors (i.e., medications, teratogens, nutrient deficiency, etc.) suggest a shared causation. Clinically, it is important to differentiate iniencephaly from other NTDs and conditions that can be treated such as nuchal tumor, Klippel-Feil syndrome (KFS) and Sprengel's deformity, etc. The fetus was evaluated by physical examination, gross measurement, observation and dissection. To examine the defects associated with iniencephaly, digital radiologic image acquisition was done using full-body x-ray films, and high-resolution CT Scans and MRI Scans. Image analysis, multi-planar reformatting, and 3D-reconstruction were done on radiographic series. A large occipital encephalocele protruded from the dorsal surface of the cranium secondary to a large defect in the occipital bone, and the frontal bone and left and right parietal bones were depressed. Severe retroflexion of the head resulting in the absence of a neck and irregular curvature of the cervical spine was seen in x-ray, CT and MRI. CT and MRI revealed esophageal atresia, renal atresia and hypoplastic lungs. The present work has characterized a case of the rare deformity, iniencephaly, with associated defects of rachischisis, cervicothoracic lordosis, esophageal atresia, hypoplastic lungs and renal atresia. This study provides insight into the early embryonic develop-

ment of a NTD and useful information for clinicians to distinguish iniencephaly from similar defects.

Key words: Human fetus – Iniencephaly – Esophageal atresia – Renal atresia – Spina bifida

Abbreviations: anterior (A); bronchi (B); carina (C); computed tomography (CT); esophagus (E); foot or inferior (F); left (L); magnetic resonance imaging (MRI); methylenetetrahydrofolate reductase (MTHFR); coronal (COR); axial (AX); sagittal (SAG); multi-planar reformatting (MPR); neural tube defect (NTD); posterior (P); right (R); three-dimensional (3D); trachea (T); weighted (Wtd); Klippel-Feil Syndrome (KFS); intrauterine growth retardation (IUGR)

INTRODUCTION

Iniencephaly is a rare and lethal NTD characterized by a triad of occipital bone defect, rachischisis, and fixed retroflexion of the head with severe cervicothoracic lordosis (Sahid et al., 2000). Blemmyes (singular: Blemmy) were first fictionalized by Pliny the Elder between 23 and 79 AD as a race of monsters without heads and necks who had eyes, a nose and mouth on their chests (Eco, 2002; Nowaczyk, 2010). Now, it is commonly thought that the inspiration for the blemmy was the birth of an iniencephalic fetus (Nowaczyk, 2010). Akin to iniencephaly, meroencephaly is a cephalic disorder that results from a NTD that occurs when the rostral neuropore of the neural tube fails to close, usually between the 23rd and 26th day of pregnancy, resulting in

Corresponding author: Ernest F. Talarico, Jr., Anatomy & Cell Biology, Indiana University School of Medicine-Northwest, Dunes Medical Professional Building, Room 3028A, 3400 Broadway, Gary, Indiana 46408-1197, USA.

Tel: 219-981-4356. E-mail: etalaric@iun.edu

Submitted: 14 March, 2013. Accepted: 21 May, 2013.

the absence of a major portion of the brain, skull, and scalp. In contrast, as the Greek word "inion" implies, the posteroinferior-most portion of the occipital bone, or occiput, is most affected in iniencephaly.

Saint-Hilare (Saint-Hilare, 1836) first described iniencephaly as associated with malformations of the central nervous system, gastrointestinal tract, respiratory system, renal system and cardiovascular system (Tugrul et al., 2007). Other associated abnormalities include hydrocephalus, encephalocele, meroencephaly, cyclopia, arthrogryposis, genu recurvatum, holoprosencephaly, omphalocele, absence of mandible, cleft lip and palate, diaphragmatic hernia, single umbilical artery, overgrowth of the arms compared to legs, and club foot (Aleksic et al., 1983; Aytar et al., 2007; Loo et al., 2001; Ramakrishnan et al., 1991). There are almost 200 cases reported in the literature (Balci et al., 2001). Patients are typically stillborn or die within hours after birth. However, there are six (rare) reported cases of relatively long-term (2-year) survival in patients with extremely mild forms of iniencephaly (Aytar et al., 2007; Kulkarni et al., 2011). Incidence varies from 0.1 to 10:10,000 (Aytar et al., 2007; Kulaylat and Narchi, 2000; Lewis, 1987), and iniencephaly is nine times more likely in female babies (Kulaylat and Narchi, 2000). Not only does iniencephaly cause obstructed labor, but it also carries the 1 - 5% risk of recurrence in subsequent pregnancies (Balci et al., 2001). The exact pathogenesis of iniencephaly is still unknown; however, there are proposed theories, most of which view the NTD from the primary neural anomaly standpoint. While no chromosomal anomalies are implicated (Balci et al., 2001), medications such as vinblastine, streptonigrin, triparano, sulphonomide, tetracycline, antihistamines, antitumor agents, and Clomiphene, and conditions including hyperhomocysteinemia and maternal diabetes have been reported to be associated with iniencephaly in humans (Bhambhani and George, 2004; Yesim et al., 2010). Differential diagnoses include meroencephaly with spinal retroflexion, Klippel–Fiel syndrome (KFS), Sprengel's deformity, nuchal tumors such as teratoma, goiter, and lymphangioma and Jarcho–Levin syndrome (Kulkarni et al., 2011).

Secondary to the wide-range of differential diagnoses that can be addressed with surgery or medical management, as well as possible causative factors and obstetrical complications, it is important that clinicians and basic scientists understand the characteristics of iniencephaly, which will lead to more accurate diagnosis and reporting, as well as to an eventual comprehensive understanding of the factors and mechanisms that result in this condition. We

report on a case of iniencephaly in a 36-week-old human female fetus discovered during anatomical dissection at the Indiana University School of Medicine-Northwest (Gary, IN), and discuss findings relative to the current literature. The application of CT and MRI technologies further clarify anomalies associated with this condition, and further differentiate this presentation from the typical case report.

MATERIALS AND METHODS

Cadaveric specimen

This study was conducted with a 36-week-old human, female fetus stored in Formal Fixx® (*Thermo Fisher Scientific*) from the gross anatomy laboratory at the Indiana School of Medicine-Northwest (IUSM-NW; Gary, IN). This fetus was placed in a jar of formaldehyde on November 7, 1957. To the best of our knowledge, this fetus had not been removed for analysis until Summer 2011. All federal and state guidelines were followed regarding the use and care of cadaveric materials, as well as all regulations set forth by the State of Indiana Anatomical Education Program.

Gross examination and photography

Detailed physical examination of fetal characteristics was done with the assistance of a local pediatric geneticist. A "Donor Report," similar to an autopsy report (Talarico, 2010, 2013) used by the IUSM-NW on adult, human cadaver donors, was adapted to record gross observations and quantitative data. Measurements done were head circumference, crown-to-rump length, crown-to-heel length, chest circumference, internipple distance, biparietal diameter, outer and inner canthal distances, ear length and position, philtrum length, palpebral fissure length, hand length, middle finger length and foot length. Digital photography of the external features was done using a NIKON D3100 SLR Camera (*B&H Foto & Electronic Corporation*, NY) equipped with an 18-55 mm VR NIKKOR Macro lens and a Nikon 40 mm f/2.8G AF-S DX NIKKOR 2200 VR Micro lens. All observations and measurements were compared with centile charts and average growth patterns seen in early human development.

X-Ray film imaging

Plain x-ray imaging was done in the radiology suite located on the second floor of the Dunes Medical Professional Building of the IUSM-NW. The following plain films were obtained: (1) anterior-posterior (AP) chest; (2) AP abdominopel-

Table 1. Age-specific item analysis and characteristics

	ASSESSMENT	ITEM	MEASUREMENTS
GESTATIONAL age	Head & Neck	Head Circumference*	20.1 cm
		Biparietal Diameter	5.6 cm
		Outer Canthal Distance	4.7cm
		Inner Canthal Distance	1.3 cm
		Ear Length	1.8 cm (R); 1.8 cm (L)
	Musculoskeletal	Philtrum Length	0.2 cm (underdeveloped without curvature)
		Palpebral Fissure Length	1.5 cm (R); 1.5 cm (L)
		Crown-to-Rump Length*	16.5 cm
		Hand Length	4.1 cm (R); 3.9 cm (L)
		Foot Length (heel-to-big toe)	5.1cm (R); 5.2 cm (L)
Thorax	Internipple Distance	3.5 cm	
GROWTH age	Musculoskeletal	Standing Height	UTP
		Supine Length	UTP
		Crown-to-Heel Length*	28.8 cm
	Thorax	Chest Circumference*	21.0 cm
	Other	Body Weight	UTP
EXTERNAL characteristics	Abdominopelvic	Genitalia	Labia major completely cover labia minora and clitoris
		Umbilical cord	2 umbilical arteries and 1 umbilical vein (dissected)
	Head & Neck	Palate	No cleft palate
		Low-set Ears	0.4 cm (R); 1.5 cm (L)
		Nose	Squashed, nares flared
		Pinna	Well-defined incurving of whole upper pinna
		Calvaria	Depressed frontal bone and parietal bones
		Mouth	No cleft lip
	Musculoskeletal	Lanugo Hair	Bilaterally present over the lateral shoulder, brachium and antebrachium
		Plantar Creases	3 creases over anterior two-thirds, and 1 crease over the anterolateral one-fourth, of the sole
		Palmar Creases	3 creases stretching medially across two-thirds of the surface
	Thorax	Nipple	
	Other	Meningoencephalocele	6.84 cm in length; 1.94 cm in diameter
Exploded Inion		2.4 (smallest) - 2.9 cm (greatest) in diameter; 6.61 cm ² (area)	
Tuft of Hair		Integument closed over lumbar region with a single tuft of hair inferior to the meningoencephalocele	

This table shows the characteristics and measurements of the fetus used to estimate gestational vs. growth age. Data was compared to values established in the literature (Robertson, 1992; Stevenson, 2006; Winter, 1988). [Abbreviations: left (L); right (R); UTP (unable to perform)]. *Items used to estimate both gestational age and growth age per established values in the literature.

vic; (3) upper extremity (pectoral girdle, brachium, antebrachium and carpus/manus); (4) lower extremity (pelvic girdle, thigh, leg and foot); (5) AP skull and lateral (Lat) skull.

Advanced medical imaging

Full-body, high-resolution CT and MRI imaging was done at Methodist Hospitals Southlake Campus (Merrillville, IN) using a 64-slice CT scanner (*General Electric Lightspeed*[®]) capable of 3-dimensional (3D) reconstruction, and an MRI scanner (*General Electric HIGH Speed MRI*). Coronal (COR), axial (AX) and sagittal (SAG) views were generated both digitally and on film. Additional MRI scans included: (a) MRI of the brain including T1-weighted (Wtd) AX and SAG; T2-Wtd AX, AX diffusion, and FLAIR AX scans; (b) MRI of the abdomen and pelvis to include T1- and T2-Wtd sequences in COR and AX planes; (c) MRI of the knees, hips, and shoulders to consist of T1-, T2-Wtd, and STIR images in at least two planes; (d) MRI of the entire spine including T1- and T2-Wtd SAG images.

Image analysis

Processing of images, creation of 3D-reconstructions, and quantitative image analysis were done using Konica PDI Viewer 1.00 V1.0R0.00 (*KONICA Minolta*, Ramsey, NJ) and TDK CDRS Dashboard V1.0.0.5 (*TDK Medical*, Minneapolis, MN) for digital x-ray films; eFILM™ Lite™ Viewer 3.0 (*Merge Healthcare*, Chicago, IL) for radiographic series from CT-Scans; and Philips iSite Viewer (*Philips iSite*, Amsterdam, Netherlands) for radiographic series from MRI Scans. Additional image analysis and reconstruction-reformatting was done using TERARECON 3.0 (*TERARECON, Inc.*, Foster City, CA) on radiographic series from CT Scans and MRI Scans.

RESULTS

Gross examination of the fetus

A human female fetus, thought to be 26-weeks gestational age, was examined during the course of training in the Summer 2011 and 2012 International Human Cadaver Prosection Program and the formal gross anatomy course at the IUSM-NW (Talarico, 2010). Physical examination and comparison to centile and development charts (Robertson, 1992; Stevenson, 2006; Winter, 1988) was done to estimate growth and gestational age. *Gestational age* is defined as a developmental age estimated by the time elapsed from the last menstrual period (unknown in the present

case) with the appearance of physical characteristics such as palmar and plantar creases, patent nares, open palpebral fissures, presence of nipples, and finger nails, etc. In contrast, growth age is a measure of *development* or *morphogenics* (i.e., body size, weight, length, psychomotor skills, etc.) expressed in terms of norms when compared to other individuals of the same gender and chronological age. The gestational age of the fetus described here was estimated to be between 36-38 weeks, and the growth age to be approximately 26 weeks. These results are summarized in Table 1.

Briefly, the fetus was dysmorphic with bilateral talipes and enlarged limbs. The chest circumference was approximately 21.0 cm (estimation was due to partial obstruction by the meningoencephalocele). Crown-to-heel length and a crown-to-rump length (Fig. 1A) were 28.8 cm and 16.5 cm, respectively. The head circumference was 20.1 cm, and the cal-

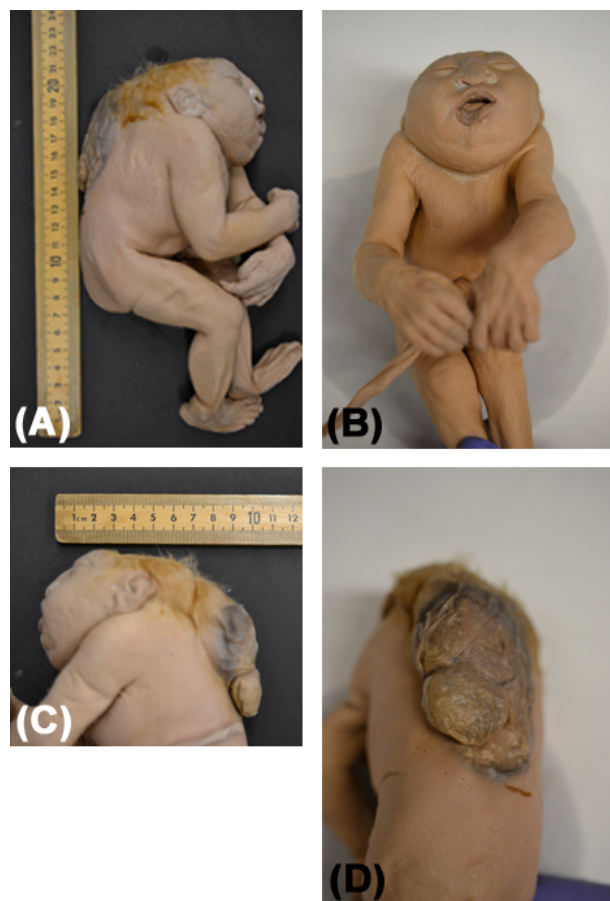


Fig. 1. Gross photography of female fetus. (A) Right lateral view of 36-38 week, gestational female fetus with crown-to-rump length of 16.5 cm. (B) Anterior view showing malformed facial features and enlarged hands and digits. (C) Left lateral view showing large meningoencephalocele draped over thoracic and lumbar spine. (D) Posterior view of meningoencephalocele.

varia had a large posteroinferior defect in the occipital bone and a severely depressed frontal bone and parietal bones (Fig. 1A-C). The meningocele was encapsulated within a thin, membranous sac (Fig. 1D), and measured 6.84 cm from its origin to terminus. A tuft of dark hair was present on the medial aspect of the dorsum inferior to the meningoencephalocele. The left and right palpebral fissures were marginally opened (Fig. 2A), and the length of the palpebral fissures, from lateral to medial canthus was 1.5 cm. Low-set ears were observed, and ear location was determined by drawing a line from the superior most border of the pinna perpendicular to a line parallel to and at the level of the lateral canthus (Fig. 2A). The helices of the right and left ears were 0.4 cm and 1.5 cm, respectively, inferior to the line drawn posteriorly from the lateral canthus of each eye (Fig. 2A). The palms had multiple creases stretching medially across the surface (Fig. 2B); digits were properly developed on both hands, and each digit had an associated fingernail located on the distal phalanx. The right foot measured 5.1 cm and the left (Fig. 2C) was 5.2 cm in length. Lanugo hair (Fig. 2D) was seen on the

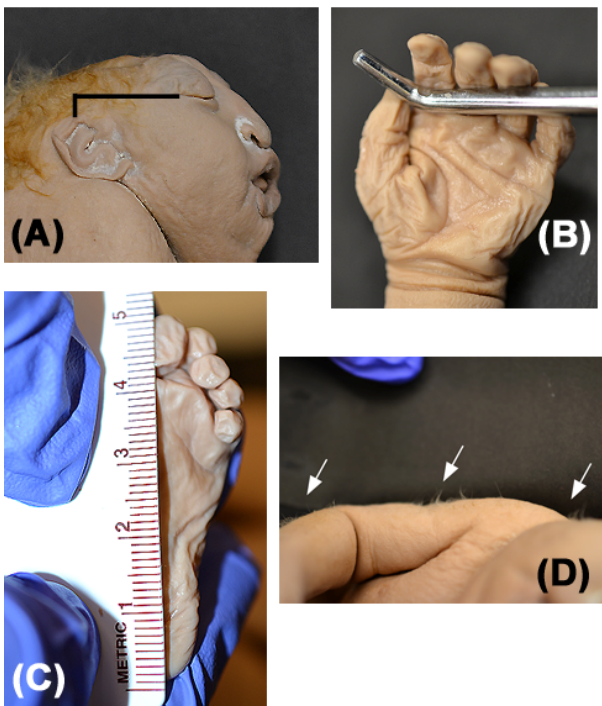


Fig. 2. Assessment of gestational characteristics. **(A)** Right lateral view of head showing lines (black) used to determine presence of low set ears. **(B)** Supinated view of left hand showing palmar creases used to estimate gestational age. **(C)** Plantar view of left foot showing full-length measurement and plantar creases. **(D)** This photograph documents the presence of lanugo hair (white arrows) in the integument over the right shoulder, brachium and antebrachium.

brachium, antebrachium, and the lateral aspect of the shoulder, bilaterally. Genital examination showed the labia majora to fully cover the labia minora and clitoris.

Medical imaging

Plain X-ray, full-body, right Lat (Fig. 3) and AP views showed that the frontal, occipital, and parietal bones were underdeveloped and malformed. Meroencephaly and rachischisis are present. The embryonic exencephalic brain shows nervous tissues with extensive degeneration. The remains of the brain appear as a spongy, vascular mass consisting mostly of hindbrain structures and meningoencephalocele. Gas can be observed in the gut (Fig. 3); a primitive rectal canal is present with patent anus. Skeletal structures are appropriate for stage of development, and bilateral talipes is present (Fig. 3).

Using a CT AX series, images at 0.25 mm slice thickness were created of the entire fetus in COR and SAG planes. Multi-planar reformatting (MPR) was used to view slices in different planes for further analysis and measurement (Fig. 4). MPR also provided information on the spinal column showing segments of abnormal cervical and thoracic curvatures (Fig. 4B). The thorax is kyphotic and there is extension in the cervical



Fig. 3. Right lateral X-ray film. The fetal specimen was imaged using plain x-ray. Note in this image the lack of density of bony structures (normal at this gestational age). The spine, meningoencephalocele, and gut tube (radiolucency) are observed. Cervicothoracic lordosis is also visible.

regions giving rise to the gross appearance (Fig. 1A-1C) of the head sitting hyperextended on a flexed cervical spine. Thus, the anatomical structures associated with the anterior portion on the cephalic region (orbits, nose and chin) are inclined (Fig. 1B and 1C; Fig. 2A; Fig. 3).

Cervicothoracic lordosis and esophageal atresia were detected in COR and SAG views and measurements of this blind-ended gut tube were

done using MPR images (Fig. 4B and C). Posterior to the trachea, the esophagus is shown extending from C3 to T5 (vertebral discs were used as reference points to clarify the boundaries of the esophagus). The esophagus measured 2.0 cm in length from proximal (i.e., pharyngeal) end to the distal, blind-ended sac (in this case the “nuchal level”). Superior to the trachea, the proximal opening of the esophagus

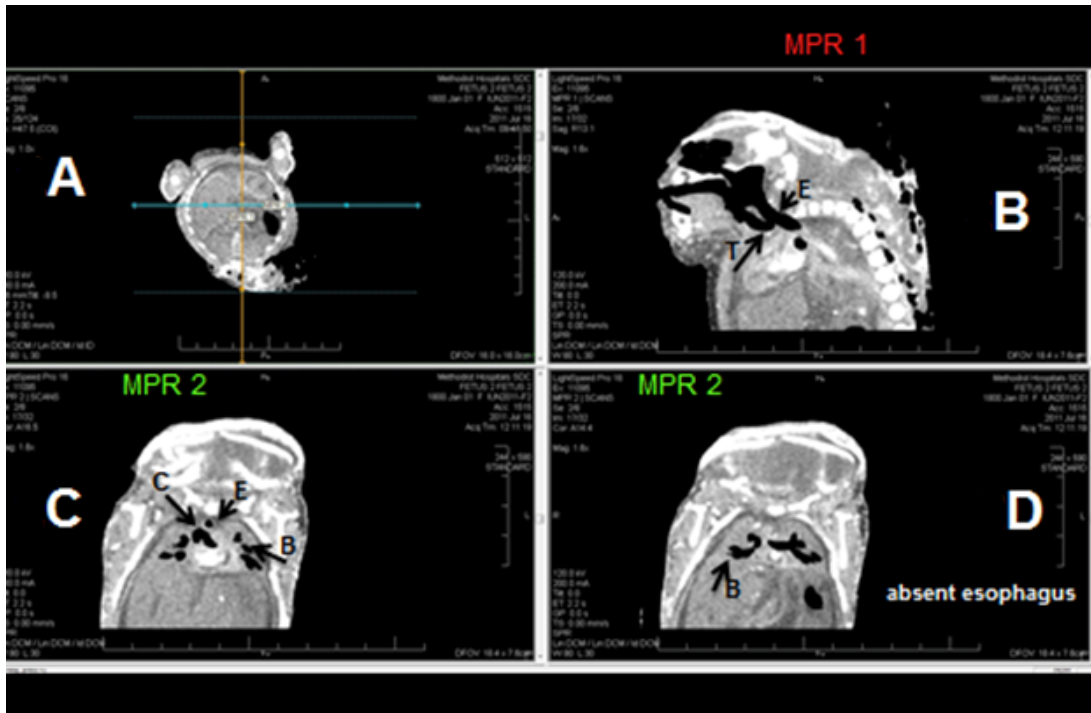


Fig. 4. Multi-planar reformatting computed tomography image analysis. Multi-planar reformatting technology was applied to axial series (A), yielding sagittal (B) and coronal (C) and (D) images. Note the trachea and esophagus in (B); carina, esophagus and bronchi in (C). Slices in this series move inferiorly (D), where the esophagus is absent. [Abbreviations: trachea (T); esophagus (E); carina (C); bronchi (B)]

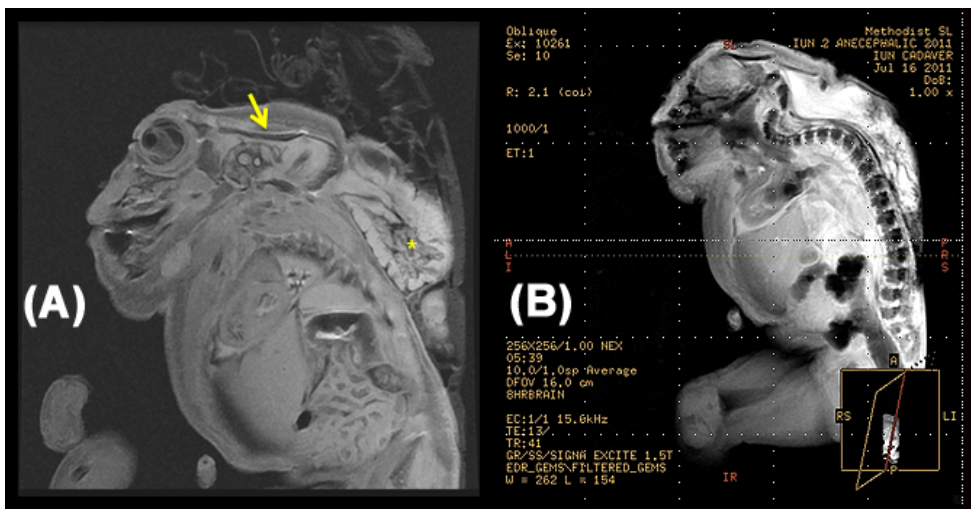


Fig. 5. Sagittal magnetic resonance imaging (MRI) of fetus. (A) MRI scan demonstrates underdeveloped calvaria (yellow arrow) with absent cerebral hemispheres. Only primitive neural tissue remains protruding into a dorsal meningoencephalocele (asterisk). Lungs are underdeveloped. (B) High-resolution, T2-weighted MRI averaging shows flatus in the gut; fluid in the meningoencephalocele and cervicothoracic lordosis.

had an AP-diameter of 0.6 cm and an AP-dimension of 0.4 cm at the level of the carina (Fig. 4C). The carina gave rise to major bronchi and esophagus became absent inferiorly (Fig. 4C vs. 4D).

Because the gantry of the MRI unit was too large for a fetus, the fetus was placed in supine position inside a head magnet, and then into the gantry to enhance image resolution. Full-body series were obtained using high-resolution 1.00 mm thick slices. MRI images reveal an underdeveloped calvaria, absent cerebral hemispheres, underdeveloped mid-brain, cerebellar hypoplasia and primitive neural tissues protruding into the meningoencephalocele from the posteroinferior defect in the occipital bone (Fig. 5). The meningoencephalocele measured 6.84 cm from caudal to rostral ends and had an AP-thickness of 1.94 cm in the cervical region. The lungs were underdeveloped and the kidneys were absent. MRI averaging (Fig. 5B) showed the severe extent of cervicothoracic lordosis and the presence of flatus in a discontinuous gut tube, as well as extension of tissue-fluid meningocele inferiorly to level L3 seen in the SAG view.

Image analysis

Dimensions of the meningoencephalocele were determined from multiple sites on the dorsum of the fetus: mid-sagittal (cervical), mid-point (thoracic), and distal (lumbar) segments, and were evaluated through CT and MRI image reformatting. These measurements define the size, shape and location of the meningoencephalocele with reducing dimensions along progressively distal measuring sites. The mid-sagittal segment, located posterior to the second/third cervical vertebrae measured 2.2 cm. The thoracic segment measured 1.4 cm, and the distal portion measured 0.9 cm. In the cervical region, the posterior aspect of the vertebrae was open and the meningoencephalocele was contiguous with a defect in the foramen magnum, which is an anomaly known as rachischisis.

CT 3D-reconstruction was used with an applied "abdomen-bubble" filter to create a "bubble" construct of the head and "neck" region (Fig. 6). This construct clearly shows the anatomical relationship of the esophagus and trachea, and supports the diagnosis of esophageal atresia showing that at 3.0 cm inferior to the esophageal terminus, only the carina and subsequent major bronchi are visible (Fig. 6 and Fig. 4B-C).

TERARECON imaging in multiple views (Fig. 7) documented defects in skeletal structures. Ab-

normally enlarged orbits are visible in the anterior view (Fig. 7A). Further, the enlarged orbit and depressed frontal bone and right parietal bone are appreciated in the right lateral view (Fig. 7R). The posterior view (Fig. 7P) and left-lateral, oblique view (Fig. 7L) document a large opening in the occipital bone of 2.9 cm maximum diameter (Table 1) continuous with the foramen magnum and inion. Further, the vertebrae along the full-length of the spinal column are open posteriorly, in contrast to a closed vertebral column expected for the determined gestational age. This supports the associated malformation of Spina bifida, and given the presence of closed skin and hair over the lumbar region, also gives evidence for Spina bifida occulta.

DISCUSSION

This study has described a case of iniencephaly in a human female fetus of gestational age 36-38 weeks. Measurements showed a difference in the gestational age versus the growth age of the fetus. This is evidence of intrauterine growth retardation (IUGR). IUGR is typically defined as less than 10 percent of predicted fetal weight for gestational age, may result in significant fetal morbidity and mortality if not properly diagnosed (Vandenbosche and Kirchner, 1998; Moh et al., 2012). This condition is most commonly caused by inadequate maternal-fetal circulation, with a resultant decrease in fetal growth. Other causes include intrauterine infections such as cytomegalovirus and rubella, and congenital anomalies. In this investigation, the growth age of this fetus was estimated to be 26

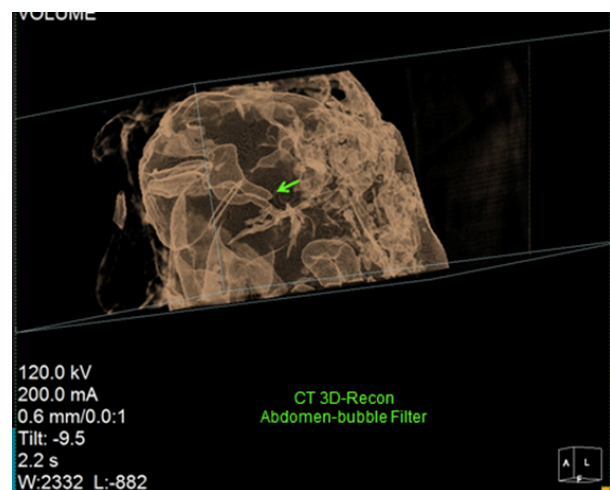


Fig. 6. CT 3D-reconstruction. Three-dimensional reconstruction with applied abdomen-bubble filter was used to generate this "bubble" construct showing esophageal atresia in this cadaveric specimen. Note the blind-ended esophagus (green arrow). [Orientation marker in lower right corner: anterior (A); left (L); foot or inferior (F)]

weeks, and lags behind that of gestational age secondary to the malformations present in association with iniencephaly. Here, these were found to be esophageal atresia, renal atresia, hypoplastic lungs, encephalocele; low set ears, occipital bone defect; cervicothoracic lordosis, depressed frontal and parietal bones, Spina bifida and club feet. Similar to the present case, David and Nixon (David and Nixon, 1976) showed that the most frequent system affected by iniencephaly is the urinary system (affected in 19% of the cases) and was followed by the cardiovascular and gastrointestinal systems each being affected in 8% of cases.

In iniencephaly, the extreme curvatures of the

cervical and thoracic regions of the vertebral column orient the head into a stargazing position that can be observed on ultrasound, where the cervical vertebrae are contiguous with the foramen magnum of the base of the skull and an “exploded” inion, and collectively form the condition known as rachischisis. Findings from this case agree with those characteristics described in previous studies such as an encephalocele pouch located at the midline of the craniocervical junction, a significantly short neck and slightly upward turned face, and overgrowth of the arms compared to the legs (Aytar et al., 2007; David and Nixon, 1976; Winter, 1988). The important features that help to diagnose inien-

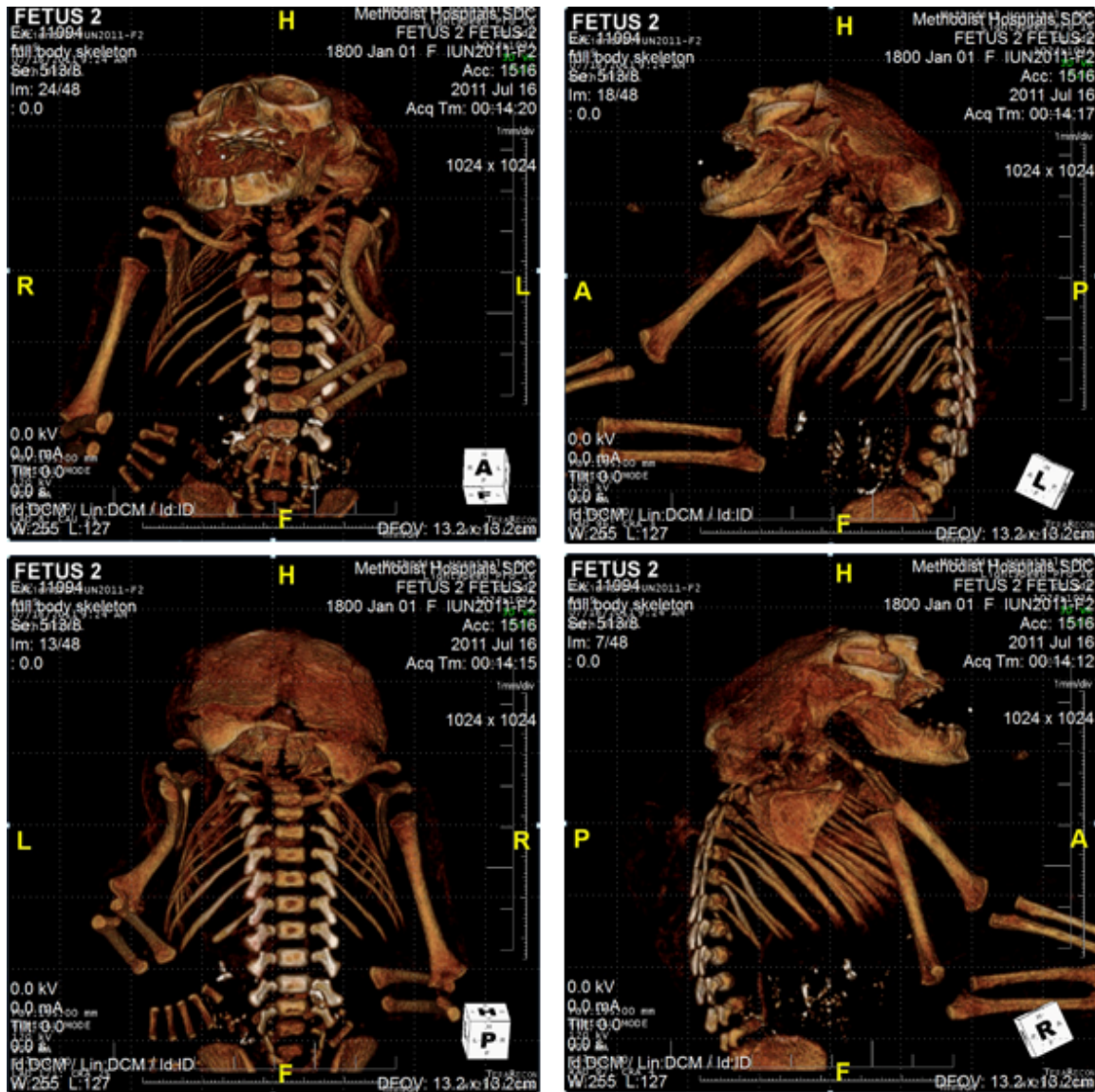


Fig. 7. TERARECON analysis. High-resolution computed tomography scans were graphically analyzed using TERARECON software generating high-resolution, 3-D skeletal reconstructions in the anterior (A); left (L); right (R); posterior (P) views and cinema (not shown). Depressed and underdeveloped frontal, parietal and temporal bones are observed. There is a large posteroinferior opening at the base of the cranial vault that is continuous with the meningoencephalocele (L and P). The orbits are enlarged. The spinal canal appears open posteriorly (P, L and R).

cephaly are as follows:

1. Occipital bone deficit leading to enlarged foramen magnum.
2. Irregular fusion of malformed vertebrae.
3. Incomplete closure of vertebral arches and bodies.
4. Retroflexion of the cervical spine.
5. Upward turned face with chin continuous with chest because of the absence of neck.

Our case had all these features in addition to other associated anomalies.

Congenital retroflexion of spine is mainly seen in two groups of anomalies: meroencephaly and iniencephaly. Two main types of iniencephaly have been classified (Cuillier et al., 2003; Lewis, 1987): "iniencephaly apertus" which has an encephalocele and "iniencephaly clausus" which has a spinal defect but no cephalocele. Clinically and anatomically, iniencephaly apertus should be differentiated from meroencephaly with retroflexion of spine, and in addition, iniencephaly clausus should be differentiated from KFS, Sprengel's deformity and cervical meningo-myelocele (Chen, 2007; Munden et al., 1993; Sherk et al., 1974).

Meroencephaly shows a total or partial absence of neurocranium and retroflexed head is not covered with skin. However, in iniencephaly the retroflexed head is completely covered with skin. Cervical vertebrae are abnormal in iniencephaly and they are almost normal in meroencephaly. In the present case the retroflexed head was completely covered with skin and a large encephalocele was present. With reference to the differential diagnosis between iniencephaly clausus and KFS, KFS is caused by a failure of segmentation of the cervical vertebrae during early fetal development. Although fusion of cervical vertebrae and malformation may be present in both, retroflexion of head is usually not seen in KFS and the presence of retroflexed head should raise suspicion of iniencephaly. Sprengel's deformity (also known as high scapula or congenital high scapula) is a rare congenital skeletal abnormality where a person has one shoulder blade that sits higher on the back than the other. The deformity is due to a failure in early fetal development where the shoulder fails to descend properly from the neck to its final position. Critically, it is important to differentiate between mild iniencephaly and KFS or Sprengel's deformity because KFS and Sprengel's deformity are not lethal and can be surgically corrected. Other entities that come in

differential diagnosis are nuchal tumors such as teratoma, goiter, lymphangioma and Jarcho-Levin syndrome.

Other findings in our case are hypoplastic lungs, cerebellar hypoplasia, and bilateral talipes. Chen in his study has found pulmonary defects in 14.3% of cases (Chen, 2007). Iniencephaly carries a bad prognosis; in only six documented cases of survival, the diagnosed patients suffered from extremely mild forms of iniencephaly in comparison to the usual phenotypic presentation of (Aytar et al., 2007; Katz et al., 1989; Munden et al., 1993).

In general, the demographic variables associated with iniencephaly parallel those of meroencephaly, and those for other NTDs associated with extra-cranial anomalies, suggesting a shared pathogenesis (Stevenson, 2006). Gardner (1979) regarded iniencephaly as "ruptured meroencephaly", this being part of his theory that rupture of the neural tube is the pathogenic mechanism in NTDs, rather than failure of the tube to close. Iniencephaly has also been attributed to an "arrest" in the embryo of the physiological retroflexion during the third week of gestation or by failure of normal forward bending during the fourth week (Pungavkar et al., 2007). Kjaer et al. (1999) found remnants of notochordal tissue in the cervical region of a 16-week gestational age fetus afflicted with iniencephaly. These remnants were observed to be located more posteriorly than normal. Further, remnants of the notochord found in the thoracolumbar region were "curled up". These observation led Kjaer's team to hypothesize that iniencephaly might arise because of deviant gene expression in the embryonic period affecting the dorsoventral orientation of the body axis, as anatomically indicated by the notochordal malpositions. Yet, in another study, application of polymerase chain reaction and allele specific digestion with Hinf-I showed a methylenetetrahydrofolate reductase (MTHFR) C677T polymorphism in the maternal parent of a 22-week-old iniencephalic female fetus (Balci et al., 2001). The mother was treated with folic acid supplementation for future pregnancies, and subsequently gave birth to a healthy boy. Although the role of MTHFR polymorphism and folate deficiency has not been clearly elucidated, carriers of this MTHFR polymorphism are at risk for hyperhomocysteinemia and maternal hyperhomocysteinemia has been associated with an increased risk of NTDs (Balci et al., 2001; Christensen et al., 1999; Ma et al., 1999). More recently, Tonni et al. (2007) also documented a case of iniencephaly associated with acrania-encephalocele, Spina bifida and abnormal ductus arteriosus in a fetus with trisomy 18 at 12-week's gestation. In

this case, the mother had a homozygous state for the MTHFR polymorphism. Finally, cases of iniencephaly and chromosome mosaicism, mosaic trisomy 13 and mosaic monosomy X, have been reported (Halder et al., 2005).

Whether notochordal malpositions, MTHFR polymorphisms, chromosomal abnormalities or medication use are causative or chance occurrences with iniencephaly is unknown. Perhaps, like other NTDs, iniencephaly could be a condition of etiopathogenetic heterogeneity. In any case, clinicians and anatomists need to be aware of iniencephaly and its associated malformations. Screening for iniencephaly can be done within the first trimester using maternal serum and amniotic alpha-fetoprotein (Balci et al., 2001; Cameron and Moran, 2009). However, ultrasonography is the modality of choice for prenatal screening and it provides cost-effective, real-time fetal images that can reveal much information about the fetus and detect major abnormalities such as iniencephaly (Cameron and Moran, 2009; Rousso et al., 2003; Sahid et al., 2000). Prenatal diagnosis may allow for elective abortion or preterm induction to avoid labor dystocia, maternal trauma during delivery and the complication associated with Caesarean section (Sahid et al., 2000). In summary, we characterize a case of iniencephaly describing anatomy and distinguishing this disorder from other treatable developmental anomalies.

ACKNOWLEDGEMENTS

The authors wish to express their sincere gratitude to the anonymous family that bequeathed the remains of their daughter for medical education and basic science research. We express our sincere appreciation to Luis O. Marquez, Director of Imaging Service, Methodist Hospitals Southlake Campus, and to Rhonda C. Doring, CT Technologist, Methodist Hospitals Southlake Campus, for their assistance in the development of radiographic materials for this case. We also thank Janice Z. Katic, M.D., Pediatric Geneticist, Clinical Associate Professor, and Director of the Indiana University School of Medicine-Northwest Genetics Center (Gary, IN) for her expertise with physical examination and diagnosis. We thank Stephen M. Koveck, Gross Anatomy Laboratory Assistant, Indiana University School of Medicine-Northwest (Gary, IN) for his assistance with photography in the early stages of this study. We also thank Dan L. Miska, Director of the Anatomical Gift Program and Anatomy Lecturer, Boonshoft School of Medicine, Wright State University (Dayton, OH) for his constructive review of this manuscript. Finally, the authors express their sincere appreciation to Charles Christopher Sheid, Coordinator of Marketing and Public Information, Western Wyoming Community College (Rock Springs, WY), for his editorial expertise.

NOTES ON CONTRIBUTORS

ERNEST F. TALARICO, JR., Ph.D., is Associate Director of Medical Education and Associate Professor of Anatomy & Cell Biology at the Indiana University School of Medicine-Northwest (Gary, IN), and is Step Master for Human Structure, and Course Director of Human Gross Anatomy, Embryology & Radiology. Dr. Talarico holds a joint appointment as Associate Faculty in the Department of Radiologic Sciences at Indiana University Northwest. He created and serves as director for the International Human Cadaver Prosection Program, which in 2008 received the award for most outstanding and innovative program in undergraduate and continuing medical education from the AAMC Central Group on Educational Affairs. He is creator of the "Talarico Protocol for Human Gross Anatomy" and is the 2008 recipient of the Partnership Matters Award from the Northwest Indiana Area Health Education Center. In recognition of his work and innovations in anatomical education, in October 2010, Dr. Talarico was inducted as a fellow into the Northwest Indiana Society of Innovators.

THEODORE M. HIEMSTRA, is a senior at Purdue University Calumet (Hammond, IN) seeking a Bachelor of Science in Biology with a minor in Chemistry. Mr. Hiemstra has been involved in anatomical research in the *Talarico Laboratories*, and has participated in the 2011 - 2013 Summer International Human Cadaver Prosection Programs. He is also an active member of Purdue University Calumet Biology Club, Chemistry and Physics Clubs, the Delta Epsilon Chi and Distributive Education Clubs of America, and is a representative of the Student Government Association.

REFERENCES

- ALEKSIC S, BUDZILOVICH G, GRECO MA, FEIGIN I, EPSTEIN F, PEARSON J (1983) Iniencephaly: a neuropathologic study. *Clin Neuropathol*, 2: 55-61.
- AYTAR MH, DOGULU F, CEMIL B, ERGUN E, KURT G, BAYKANER K (2007) Iniencephaly and long-term survival: a rare case report. *Childs Nerv Syst*, 23: 719-721.
- BALCI S, AYPAR E, ALTINOK G, BODUROGLU K, BEKSAC MS (2001) Prenatal diagnosis in three cases of iniencephaly with unusual postmortem findings. *Prenat Diagn*, 21: 558-562.
- BHAMBHANI V, GEORGE S (2004) Association of clomiphene with iniencephaly. *Indian Pediatr*, 41: 517.
- BOS CA, BALJET B (1999) Cynocephali and Blemmyae. Congenital anomalies and medieval exotic races. *Nederlands tijdschrift voor geneeskunde*, 143: 2580-2585.
- CAMERON M, MORAN P (2009) Prenatal screening and diagnosis of neural tube defects. *Prenat Diagn*, 29: 402-411.
- CHEN CP (2007) Prenatal diagnosis of iniencephaly. *Taiwan J Obstet Gynecol*, 46: 199-207.
- CHRISTENSEN B, ARBOUR L, TRAN P, LECLERC D, SABBAGHIAN N, PLATT R, GILFIX BM, ROSENBLATT DS, GRAVEL RA, FORBES P, ROZEN R (1999) Genetic polymorphisms in methylenetetrahydrofolate reductase and methionine synthase, folate levels in red blood cells, and risk of neural tube defects. *Am J*

- Med Genet*, 84: 151-157.
- CUILLIER F, KOENIG P, LAGARDE L, CARTAULT JF (2003) Transvaginal sonographic diagnosis of iniencephaly apertus and craniorachischisis at 9 weeks' gestation. *Ultrasound Obst Gyn*, 22: 657-658.
- DAVID TJ, NIXON A (1976) Congenital malformations associated with and iniencephaly. *J Med Genet*, 13: 263-265.
- ECO U (2002) *Baudolino*, Pp 521. Translated from the Italian by Weaver W. Harcourt, Inc., New York.
- GARDNER WJ (1979) Klippel-Feil syndrome, iniencephalus, anencephalus, hindbrain hernia and mirror movements: overdilatation of the neural tube. *Child Brain*, 5: 361-379.
- HALDER A, AGARWAL S, PANDEY A (2005) Iniencephaly and chromosome mosaicism: a report of two cases. *Congenit Anom (Kyoto)*, 45: 102-105.
- HUNTER AGW (2006) Brain and Spinal Cord. In: *Human Malformations and Related Anomalies*, 2nd Edition. Chapter 16. Oxford University Press, New York.
- KATZ VL, AYLSWORTH AS, ALBRIGHT SG (1989) Iniencephaly is not uniformly fatal. *Prenat Diagn*, 9: 595-599.
- KJAER I, MYGIND H, FISCHER HANSEN B (1999) Notochordal remnants in human iniencephaly suggest disturbed dorsoventral axis signaling. *Am J Med Genet*, 84: 425-432.
- KULAYLAT NA, NARCHI H (2000) Iniencephaly: an uncommon neural tube defect. *J Pediatr*, 136: 414.
- KULKARNI PR, RAO RV, ALUR MB, JOSHI SK (2011) Iniencephaly clausus: a case report with review of literature. *J Pediatr Neurosci*, 6: 121-123.
- LEWIS HF (1987) Iniencephalus. *Am J Obstet Gynecol*, 35: 11-53.
- LOO CK, FREEMAN B, STANFORD D (2001) CNS findings in iniencephaly: case report and literature review. *Pathology*, 33: 112-115.
- MA J, STAMPFER MJ, CHRISTENSEN B, GIOVANNUCCI E, HUNTER DJ, CHEN J, WILLETT WC, SELHUB J, HENNEKENS CH, GRAVEL R, ROZEN R (1999) A polymorphism of the methionine synthase gene: association with plasma folate, vitamin B12, homocyst(e)ine, and colorectal cancer risk. *Cancer Epidemiol Biomarkers*, 8: 825-829.
- MOH W, GRAHAM JR., JM, WADHAWAN I, SANCHEZ-LARA PA (2012) Extrinsic factors influencing deformations and intrauterine growth restriction. *J Pregnancy*, Article ID 750485, 1-11, <http://www.hindawi.com/journals/jp/2012/750485/>
- MUNDEN MM, MACPHERSON RI, CURE J (1993) Iniencephaly: 3D-computed tomography imaging. *Pediatr Radiol*, 23: 572.
- NORMAN MG, MCGILLVRAJ BC, KALOVSEK DK, HILL A, POSKITT J (1995) *Congenital Malformations of the Brain: Pathological, Embryological, Clinical, Radiological and Genetic Aspects*. Oxford University Press, New York.
- NOWACZYK MJM (2010) The Blemmye: A Medieval Grotesque Inspired by Iniencephaly? *Am J Med Genet*, 152 (Pt A): 1583-1585.
- PUNGAVKAR SA, SAINANI NI, KARNIK AS, MOHANTY PH, LAWANDE MA, PATKAR DP, SINHA S (2007) Antenatal diagnosis of iniencephaly: sonographic and MR correlation: a case report. *Korean J Radiol*, 8: 351-355.
- RAMAKRISHNAN S, SHARMA DC, RAMAKRISHNAN V, PARIHAR PS, SHARMA S, KANTHER DK (1991) Iniencephaly with cyclopi (a case report). *J Postgrad Med*, 37: 51-52, 52A.
- ROBERTON NRC (1992) *Textbook of Neonatology*. 2nd Edition, Churchill Livingstone, United Kingdom.
- ROUSSO D, PSARA A, VENIZELOS I, TSIMAS V, KOURTIS A, PANIDIS D (2003) Prenatal ultrasonographic diagnosis of iniencephaly. *J Obstet Gynaecol*, 23: 572-573.
- SAHID S, SEPULVEDA W, DEZEREGA V, GUTIERREZ J, RODRIGUEZ L, CORRAL E (2000) Iniencephaly: prenatal diagnosis and management. *Prenat Diagn*, 20: 202-205.
- SAINT-HILARE IG (1836) *Historie des anomalies del organization*. 1st Edition 2. In: Balci S et al. (2001) Prenatal diagnosis in three cases of iniencephaly with unusual postmortem findings. *Prenat Diagn*, 2021: 2558-2562.
- SHERK HH, SHUT L, CHUNG S (1974) Iniencephalic deformity of the cervical spine with Klippel-Feil anomalies and congenital elevation of the scapula. *J Bone Joint Surg*, 56 (Pt 3A): 1254-1259.
- SOGAARD K, SKIBSTED L, BROCKS V (1999) Acardiac twins: pathophysiology, diagnosis, outcome and treatment. Six cases and review of the literature. *Fetal Diagn Ther*, 14: 53-59.
- STEVENSON RE, HALL JG (2006) *Human Malformations and Related Anomalies*, 2nd Edition. Oxford University Press, New York.
- TALARICO EF, JR (2010) A human dissection training program at Indiana University School of Medicine-Northwest. *Anat Sci Educ*, 3: 77-82.
- TALARICO EF, JR (2013) A change in paradigm: giving back identity to donors in the anatomy laboratory. *Clin Anat*, 26: 161-172.
- TONNI G, AZZONI D, PANTEGHINI M, VENTURA A, CAVALLI P (2007) First trimester diagnosis of iniencephaly associated with fetal malformations and trisomy 18: report of a new case and gene analysis on folate metabolism in parents. *Congenit Anom (Kyoto)*, 47: 101-104.
- TUGRUL S, ULUDOGAN M, PEKIN O, USLU H, CELIK C, ERSAN F (2007) Iniencephaly: Prenatal diagnosis with postmortem findings. *J Obstet Gynaecol Re*, 33: 566-569.
- VANDENBOSCHE RC, KIRCHNER JT (1998) Intrauterine growth retardation. *Am Fam Physician*, 58: 1384-1390.
- WINTER RM, KNOWLES SAS, BIEBER FR, BARAITSER M (1988) *The Malformed Fetus and Stillbirth: A Diagnostic Approach*. John Wiley & Sons, New York.
- YESIM A, HABIBE A, OYA D, DAVUT S, ERSAN D, HAMDULLAH S, MEHMET U (2010) Iniencephaly with mediastinal bronchogenic cyst: a case report. *J Prenat Med*, 4: 74-76.